J Mater Sci (2008) 43:5763–5771
DOI 10.1007/s10853-008-2878-5

Eco-composite developed using biomorphous stiff skeleton of carbonised yucca and furfuryl alcohol as a filler

M. Krzesińska · J. Zachariasz · A. I. Lachowski · Ł. Smędowski

Received: 10 April 2008 / Accepted: 14 July 2008 / Published online: 9 August 2008

Abstract The aim of this research was to prepare a monolithic porous carbon–carbon composite on the basis of porous stiff skeleton obtained via carbonisation of blocks cut from horticultural waste, lignified inflorescence stems of yucca, *Yucca flaccida.* Then the blocks were infiltrated by furfuryl alcohol, polymerised, cross-linked and carbonised. Raw yucca carbonised at various temperatures and the resultant ecological composites were characterised using the following methods: helium gas densitometry, ultrasonic and electrical resistance measurements, the physical adsorption of N_2 gas at −196 °C, scanning (SEM) and transmission (TEM) electron microscopies. Elemental analysis, i.e. the CHN content and organic constituents, were determined for raw yucca. The thermal decomposition of composites and their precursors were investigated at temperatures ranging from 20 to 940 °C using thermogravimetric analysis (TGA). The composites were found to be highly porous carbon materials thermo-resistant in inert atmosphere with a strong skeleton and hierarchically ordered structures. Their elastic and electrical properties were found to be anisotropic and dependent on the support properties.

M. Krzesińska (✉) · J. Zachariasz
Centre of Polymer and Carbon Materials, Polish Academy of Sciences, Marii Curie-Skłodowskiej 34, 41819 Zabrze, Poland
e-mail: marta.krzesinska@cmpw-pan.edu.pl

M. Krzesińska · Ł. Smędowski
Department of Electron Technology, Institute of Physics, Silesian Technical University, Krzywoustego 2, 44100 Gliwice, Poland

A. I. Lachowski
Institute of Chemical Engineering, Polish Academy of Sciences, Baltycka 5, 44121 Gliwice, Poland

Introduction

Wood and plant-based materials, bio-plastic, bio-ceramics, wood ceramics, soil ceramics, etc. [1–15] are materials of green environmental profile. They are obtained from renewable resources and possess lower environmental burden than materials obtained from depleting minerals and fossil fuels. New porous carbon materials are obtained via carbonising wood or woody materials followed by impregnation with various resins. Wood precursors of infinite varieties are available providing different densities and pore morphologies, different levels of anisotropy, etc., and allowing a diversity of opportunities for material selection. The cellular anatomy of naturally grown plants provides an attractive template or matrix for the design of materials with hierarchically ordered structures that cannot be processed by conventional processing technologies [13]. The porous carbon materials could be used alone (active carbons, adsorbents) or in combination for filtration systems and catalyst support structures and sensors [14, 15]. Practical implementations of wood-based materials such as electromagnetic shield materials, heater for floor heating and humidity sensors have been explored. They have also been involved in the development of high-temperature absorbers. Materials produced from by-products or the waste in technical processes also reduce the environmental burden. They consume fewer resources from the eco-sphere, and reduce the substances released to eco-sphere. Thus, searching of new materials based on the Nature sources, particularly based on the waste, is very important in respect to protection of natural environment.

Lignified stems of plants carbonised at proper temperatures are expected to be promising supports, as porous stiff skeletons, for the monolithic, biomorphous composites and as biotemplates for various biomorphous ceramics. Most of

the studies cited in the literature involved materials based on carbonised woods, which vegetate 20–30 years for softwoods and 40–60 years for hardwoods. It would be useful to prepare novel materials from varieties of plants with distinctly shorter period of renewal than that of long-growing plants. Amongst short-time renewable plants, mostly bamboo was used for the manufacture of composites [16–19]. For the preparation of those biocomposites, bamboo was used generally as a source of fibres or powders, which were natural fillers of the polymer matrices. Obtaining biomorphous composites by coating internal surfaces of stiff-carbonised plant skeletons with polymer is rather rare. Figure 1 shows different structures of composites of carbonised plants used either as a filler or as a matrix (stiff skeleton).

To our knowledge, there are no publications concerning eco-composites with yucca as a precursor. Yucca (*Yucca flaccida*) belongs to the category of perennial plants; it is a flowering plant of the Agavaceae family. Dry inflorescence stems of yucca collected every year after the florescence are horticultural waste. Inflorescence stems, dry and lignified after coming out of bloom, possess a homogenous profile and vessel distribution with no branches or seasonal rings. The homogeneity of such a stem can be important because of possible applications.

In our previous papers we described pyrolysis of vascular plants such as bamboo and yucca and presented some physical properties of resulting porous carbons [20–23]. They were admitted to be promising support for various composites.

In the past we presented composites produced from compressed-expanded graphite as a support and polyfurfuryl alcohol (PFA) as a filler [24]. The resultant materials were monoliths structured as a graphite backbone coated by a thin layer of carbonised cross-linked PFA. Their conductive and elastic properties were found to be very good. Those carbon–carbon composites were expected to have interesting applications as adsorbents, and as catalyst supports. It would be useful to replace the expanded graphite support with an ecological renewable support i.e. with carbonised plant leaving PFA as a filler.

The aim of the present study was to develop biomorphous block composites using the porous carbons derived from yucca (*Yucca flaccida*) as a support (stiff skeleton) and carbonised cross-linked PFA as a filler, and to study the physical properties of the resultant composites. The first partial results were presented in [25].

Experimental

Preparation of samples

Cylindrical pieces of about 2.5–3 cm in length and 1.5–2 cm in diameter cut from woody dry stems or cuboids were used for pyrolysis. The block samples were heated under a gas flow of nitrogen (about 0.1 L/min) at temperature varying from 20 °C to the final temperature, T_c, ranging from 300 to 950 °C. The rate of heating was constant for all final temperatures and equalled to 3 °C/min. The samples were held for 1 h at the desired temperature. Weight loss during the pyrolysis ranged from 57% to 72% for increasing T_c from 300 to 950 °C. The block samples of porous carbons obtained at the final temperatures, 350 and 950 °C, were impregnated under vacuum by furfuryl alcohol (99%) in Epovac apparatus using one-step infiltration. Next, the samples were dried in the air for an hour and soaked in the solution of hydrochloric acid (2%) for 6 h. After the impregnation and polymerisation, the samples were dried in the air for an hour and then in the dryer in the temperature range 80–120 °C for 7 h. The resultant composites were carbonised under nitrogen with the constant heating rate of 3°/min to the temperature 550 °C and kept at this temperature for an hour. Composites were denoted as YT_c/FAHCL, where Y and FAHCL are abbreviations of yucca and furfuryl alcohol polymerised with HCl, respectively, while T_c is the final temperature of the yucca carbonisation mentioned above. Figure 2 shows shapes of raw yucca, carbonised plant, and the composite.

Monolithic block samples of yucca both raw and carbonised as well as of the resultant composites were

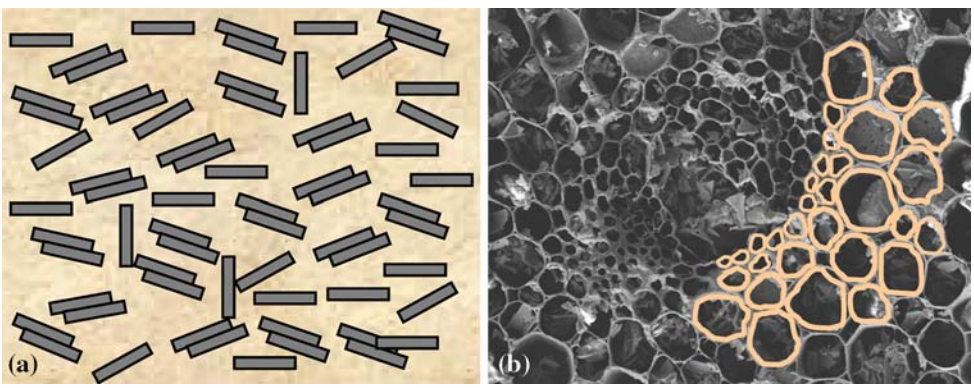

Fig. 1 Cross section of two different models of two-component composites with carbonised plant: short fibres (**a**) as a filler, flooded in continuous polymer matrix, and (**b**) carbonised plant stiff skeleton (matrix), covered by thin layer of polymer (filler). In (**b**), polymer layers are shown only on some pores of transverse section of carbonised plant

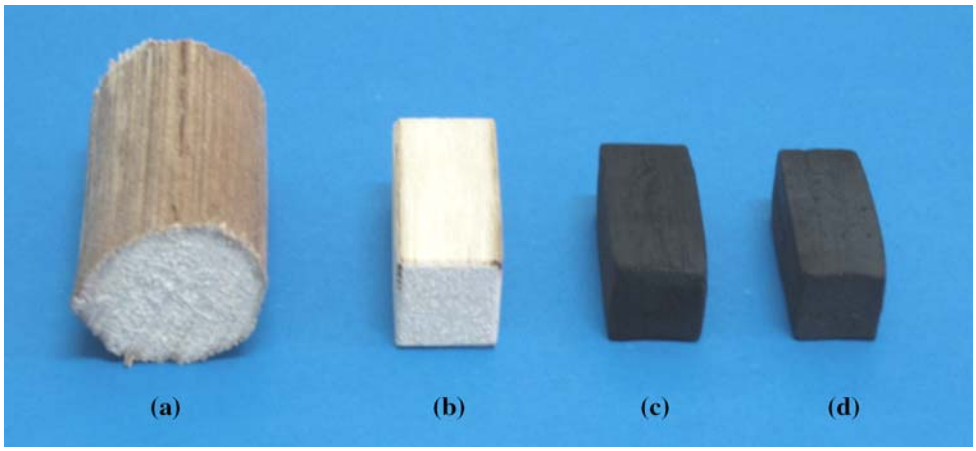

Fig. 2 Photo of the shapes of yucca raw (a piece of natural stem (**a**) and a cuboid obtained from turning the stem (**b**)), carbonised (**c**) and the composite (**d**)

characterised using various methods: thermogravimetric analysis (TGA), helium gas densitometry, the low-temperature adsorption of N_2 gas, the ultrasonic and electrical measurements, scanning (SEM) and transmission (TEM) electron microscopies. The block samples underwent ultrasonic and electrical measurements, helium gas densitometry and SEM observations, while for the elemental analysis, the TGA, TEM and the pore size distribution studies, the samples were ground.

The CHN analysis (carbon, hydrogen and nitrogen content) was made with the Perkin Elmer 2400 Series II CHNS/O System. Raw yucca was found to contain: 45.21 wt.% of carbon, 5.99 wt.% of hydrogen and 0.15 wt.% of nitrogen. The main organic constituents of raw yucca were determined by the wet-chemical analysis of organic matter method. It was found that yucca consists of 44.8 wt.% of cellulose, 16.6 wt.% of hemicellulose and 35.9 wt.% of lignin.

Characterisation of the support and the resultant composite

The TGA technique was applied for the thermal characterisation. Thermogravimetric studies were carried out with the thermogravimetric analyser TGA type Q-1500, MOM Budapest in pure nitrogen with a flow rate of 10 L/h, like in the case of carbonisation. The samples were heated from 20 to 940 °C at a heating rate of 10 °C/min.

The bulk porosity of the samples studied was calculated using the equation:

$$P(\%) = \frac{d_{\text{true}} - d_{\text{app}}}{d_{\text{true}}} \cdot 100 \quad (1)$$

where P is the bulk porosity, and d_{true} and d_{app} are the true and apparent densities of the sample, respectively. The true density was measured using the helium gas-displacement pycnometer type 1305 Micromeritics®, while the apparent density was determined from weight and volume, the latter was calculated using sample dimensions.

The mesopore size distribution of materials studied was measured by means of the adsorptive method. The adsorption of N_2 at liquid nitrogen temperature (−196 °C) was achieved on small samples using the standard volumetric apparatus ASAP 2000 (Micromeritics®). Every sample was degassed in vacuum under the pressure of about 5 μm Hg, at 140 °C for 120 h. The adsorption/desorption isotherms of nitrogen were determined point-to-point by discontinuous introduction of adsorbate into the sample holder. A number of adsorption and desorption points were performed for relative pressures in the range 0.05–0.99. The pore (mesopore) size distribution and average diameter of pores D_{DES} were calculated using the Barrett–Joyner–Halenda method.

The velocity of longitudinal ultrasonic waves at the frequency of 100 kHz was measured along parallel, v_{ax} (axial direction) and perpendicular, v_{rad} (radial direction) to the stem/fibre directions, using the ultrasonic tester (Tester CT1, UNIPAN-ULTRASONIC, Poland). Ultrasonic velocities for both parallels and perpendiculars to plant fibres were measured for yucca before and after the carbonisation, as well as for the resultant composite. Ultrasonic velocities (v_{ax} and v_{rad}) and apparent densities, d_{app}, were used for the determination of the dynamic elastic moduli E_{ax} and E_{rad} as follows:

$$E_{\text{ax/rad}} = d_{\text{app}} \cdot v_{\text{ax/rad}}^2 \quad (2)$$

Using multimeter FLUKE 8060A, electrical resistivity was measured along axial (ρ_{ax}) and radial (ρ_{rad}) directions for yucca carbonised at 350 and 950 °C as well as for composites produced using these supports.

The structure of raw and carbonised yucca was observed at various temperatures for the set of block samples along axis of the stem and perpendicularly to it, using scanning electron microscope, Zeiss, with magnification up to ×5000.

The samples of yucca carbonised at two final temperatures, i.e. at 350 and 950 °C, were selected for the TEM studies. They were poured over by ethanol and next ground

down in a mortar. Then the preparations were placed in ultrasound bath to split aggregates. The obtained suspension was put on a cooper grid covered with 'carbon film'. When alcohol had evaporated, the preparations were placed in the microscope column and analysed. The microscopic observations were carried out using PHILIPS EM400T with magnification ×23,000 and acceleration voltage 100 kV. The samples were analysed using 002 dark field technique of observation (002DF).

Results and discussion

The thermal decomposition of yucca and of the composite Y350/FAHCL was investigated using the TGA analysis. Figure 3a shows the DTG curve (the first derivative of weight loss plotted vs. temperature) determined for raw yucca in both air and nitrogen atmosphere. The first endotherm, at 90 °C, corresponds to loss of adsorbed water, while the second one at 330 °C in nitrogen (that is related to peak at 280 °C in air) is responsible for decomposition of cellulose. Unlike in solid iron bamboo [21, 23], the peak corresponding

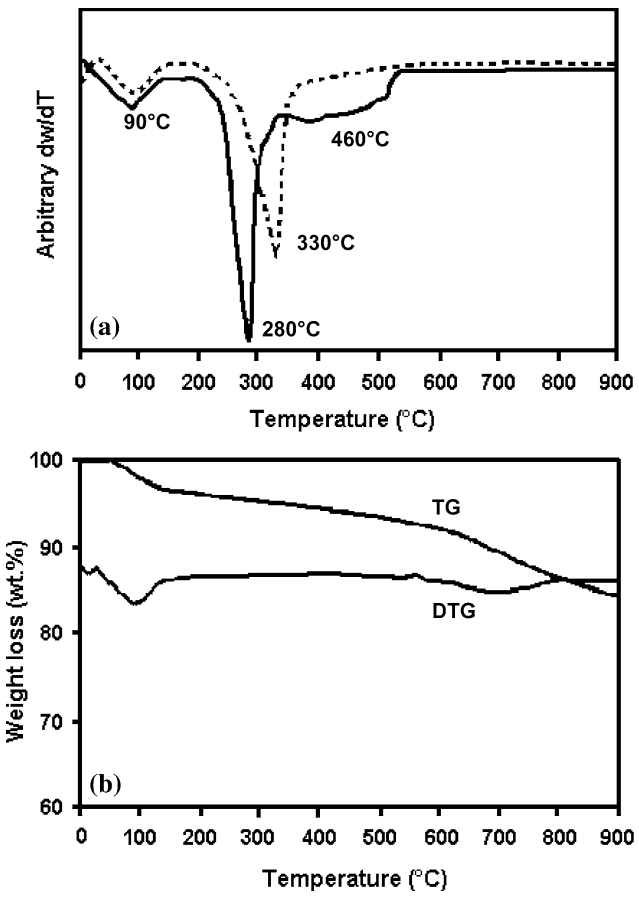

Fig. 3 The DTG thermogram of raw yucca determined in air (*solid line*) and nitrogen (*dashed line*) (**a**), and the thermogram (TG and DTG) of the composite Y350/FAHCL determined in nitrogen (**b**)

to decomposition of hemicelluloses was not observed. In yucca, the cellulose content was found to be dominated (44.8 wt.% of cellulose in comparison with 16.6 wt.% of hemicellulose), while in solid iron bamboo, content of those constituents was similar (29.4 wt.% of cellulose and 21.4 wt.% of hemicellulose). Thus, the small height peak for hemicellulose could be covered by strong signal from cellulose. On the other hand, the temperature ranges of both cellulose and hemicelluloses decomposition could be similar in yucca, giving an overlap of corresponding endotherms. The peak responsible for the thermal decomposition of lignin was found in the DTG curve detected in air, at the temperature of 460 °C. Lignin is important constituent of yucca—its content is 35.9 wt.%. Lignin as highly branched polymer composed of many various monomeric units usually degrades at temperatures in a wide range, i.e. of 280–500 °C [13]. Thus, the temperature 460 °C of the peak observed in the DTG curve, attributed to lignin, places within this range. Figure 3b shows the thermogram for the composite Y350/FAHCL. The thermogravimetric studies of this composite showed a wide and very shallow minimum in the DTG curve at around 690 °C, that can be attributed to the residual decomposition of the support, i.e. of plant previously carbonised at 350 °C (such process was observed in the case of bamboo [23]), as well as of the filler, previously carbonised at 550 °C. Figure 3b confirms that this residual decomposition is very low. This makes the composite suitable for application at high temperatures (in oxygen-absent atmosphere).

As it was shown in Fig. 3a the thermal decomposition of cellulose was finished at about 350 °C and of lignin at about 500 °C. There is a question, whether all structural changes of heat-treated yucca were finished at $T \sim 500$ °C. Cheng et al. [26] have investigated the bamboo structure under heat treatment. This plant belongs to vascular plants as yucca. The raw bamboo samples were carbonised at 800 °C and then they were heat treated at 1300 °C and graphitised at very high temperatures, 2100–3000 °C. After heat treatment up to 3000 °C the shapes and sizes of bamboo charcoal samples were hardly changed, but their weight decreased to a small extent (∼9%). Although emission of volatile matter was inconsiderable, evolution of the carbonised material structure was continued, that was confirmed by not only the samples sizes, but also by the XRD profiles. Thus, the thermogravimetric studies are not sufficient to describe all changes in the plant stem structure during heating. Therefore, the other techniques and the carbonisation temperatures higher than those of the thermal decomposition range are needed.

Figure 4 presents the bulk porosity of initial yucca and the char produced at various T_c. Carbons derived from yucca are distinctly more porous in comparison with their precursor. Incoming very high bulk porosity of about 90%

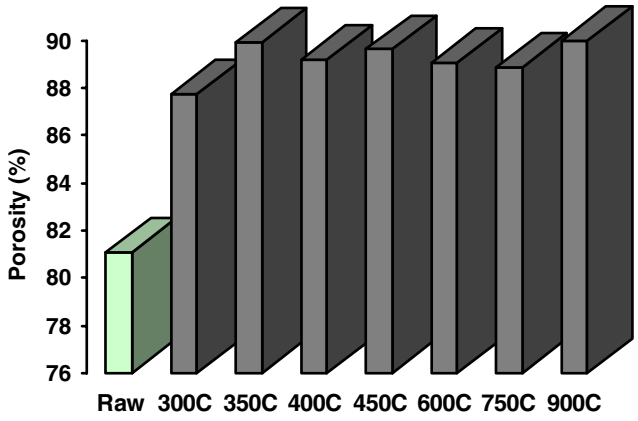

Fig. 4 The bulk porosity of raw and carbonised yucca plotted for the carbonisation temperatures studied

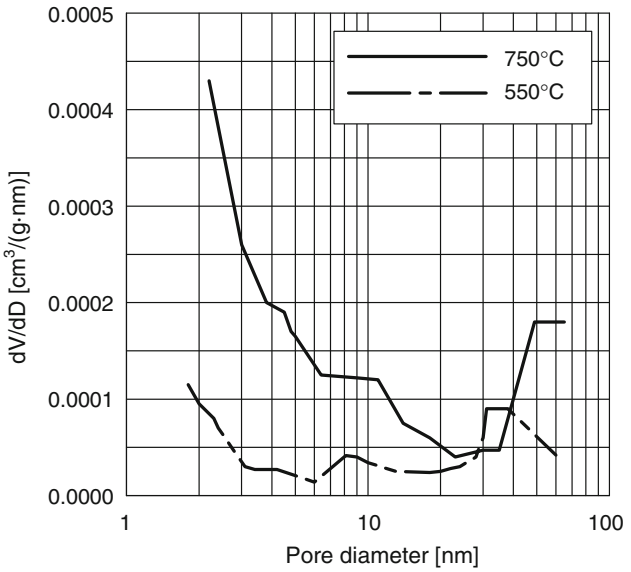

Fig. 5 Pore volume size distributions, *dV/dD*, of yucca carbonised at 550 °C (*dashed line*) and at 750 °C (*solid line*) determined (per gram of a sample) by nitrogen gas adsorption method

was already achieved for the low-temperature carbonisation product. Higher temperatures of pyrolysis slightly affected the bulk porosity.

Figure 5 shows the pore volume size distribution for yucca carbonised at two temperatures, 550 and 750 °C. It can be seen from this figure that heat treatment of yucca at 550 °C (in nitrogen atmosphere) produced pores of mean diameters of about 4.5, 8.2 and 32–38 nm. Further heating up to 750 °C caused production of next pores characterised by similar ranges of mean diameters, generally higher than those of yucca carbonised at 550 °C, i.e. they were: ~5, 11 and 50 nm. It was found that the mesopore volume increased considerably with temperature of carbonisation. Pore size distribution determined for material carbonised at 750 °C evidenced that higher temperature of carbonisation increased a number of small pores of diameters of about 1–2 nm.

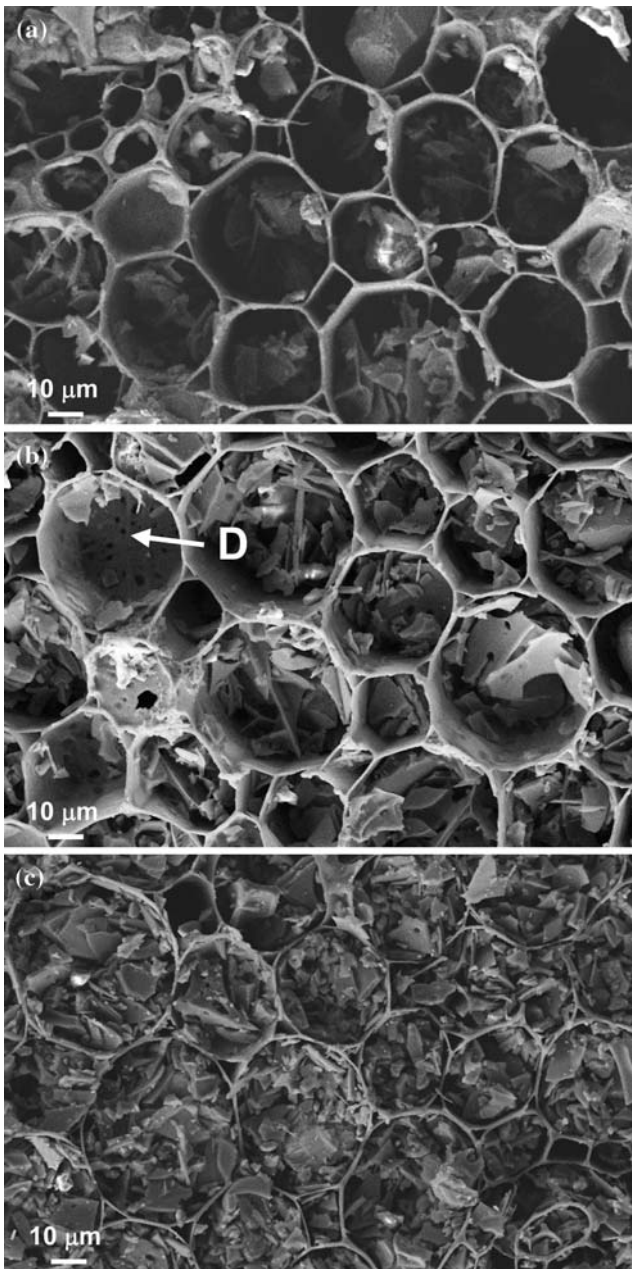

Fig. 6 SEM images of transverse sections of yucca carbonised at 550 °C (**a**), at 750 °C (**b**) and at 950 °C (**c**); magnification ×2000; D—a transverse diaphragm

Figure 6a–c shows the comparison of SEM images of transverse sections of yucca carbonised at 550, 750 and at 950 °C. Details of structure consisting of sclerenchyma cells (fibrils) parallel to the stem axis can be seen. Fibrils aligned along the stem axis are characterised by various diameters. These fibrils are arranged in honeycomb pattern, separated by thin walls of matrix. Unlike as in the case of solid iron bamboo (*Dendrocalamus strictus*) [21, 23], it was found that the degree of the thermal decomposition at given temperature was the same for all constituents

of the stem structure of yucca. Microscopic observations confirmed, similarly as it was previously reported for two kinds of bamboo [20, 21, 23], that the original cellular skeleton of yucca stem was retained in the porous carbon material during carbonisation process, although internal cell structure was changed under heat treatment. It can be seen from Fig. 6a that for lower T_c the plant tissue skeleton was characterised by empty fibrils. Higher temperatures of carbonisation caused filling of the inside volume of empty fibrils by products of the thermal destruction of transverse diaphragms present within fibrils. In the case of the highest T_c, i.e. at 950 °C, fibrils were tightly filled by more disintegrated grains arising from diaphragms, and thickness of walls was distinctly lower in comparison with the products of pyrolysis at lower T_c. It can be seen from Fig. 6 that yucca can be very useful support for eco-composites because of great empty space accessible to filler. It is obvious, that such structures, dependent on the temperature of pyrolysis, will influence the yield of infiltration of porous support by liquid filler.

Porous supports for composites have to be strong skeletons to avoid defects of the composite structure. The ultrasonic velocity is a parameter reflecting the structure stiffness. Figure 7 shows the ultrasonic velocity determined along basic directions in raw yucca and char produced at various T_c. As it can be seen from this figure, the thermal decomposition of yucca at low temperatures decreased the ultrasonic velocity, because the char was characterised by higher bulk porosity (see Fig. 4). It is known that the presence of additional pores decreases the ultrasonic velocity. Further heating up to 750 °C increased the value of the ultrasonic velocity showing substantial increase in rigidity of carbonised yucca skeleton. Pyrolysis at higher temperatures formed much stiffer char than that obtained at lower temperatures.

As it was mentioned previously, the structures shown in Fig. 6 can influence the yield of the liquid filler infiltration.

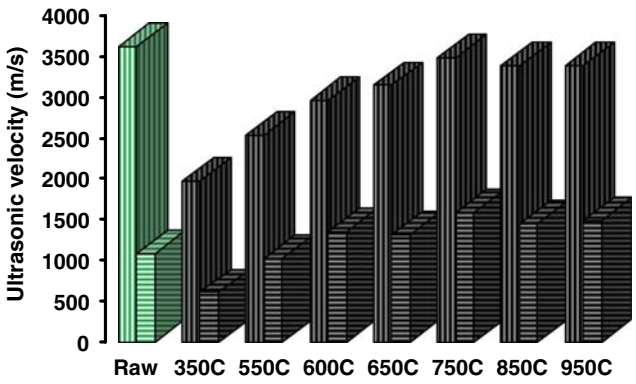

Fig. 7 The ultrasonic velocity in yucca raw and carbonised at various temperatures—left columns: axial direction; right columns: radial direction

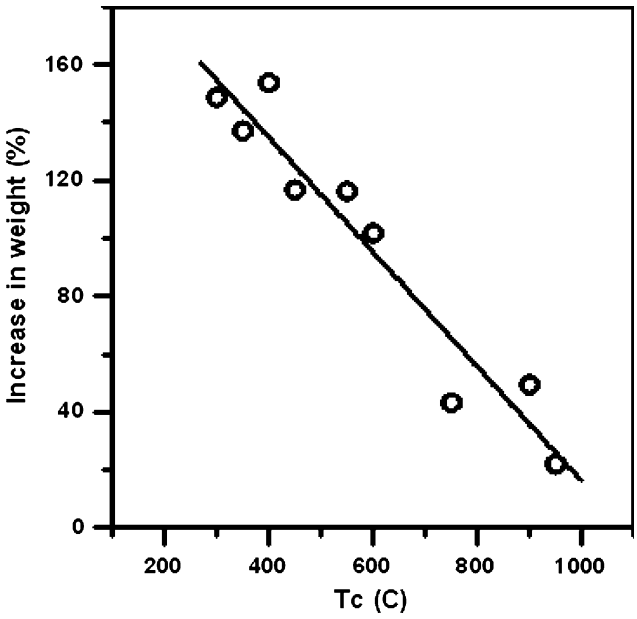

Fig. 8 The plot of increase in weight of a sample after one-step infiltration with furfuryl alcohol versus the carbonisation temperature of a support; correlation coefficient $r = 0.93$

Figure 8 shows an increase in weight of porous carbonised yucca after one-step infiltration with furfuryl alcohol plotted versus the carbonisation temperature, T_c, used for production of the supports. Degree of filling of porous support by liquid filler decreased linearly (correlation coefficient $r = 0.93$) with increasing temperature of the yucca carbonisation.

Table 1 shows the densities and the bulk porosity of raw plant stem, porous supports and the composites Y350/FAHCL and Y950/FAHCL. The empty space in highly porous carbonised yucca characterised by P of over 89% was filled partly by filler—furfuryl alcohol, that resulted in materials of lower porosity of about 73% and 83%. The reduction of the bulk porosity in the case of the low-temperature support (Y350/FAHCL), characterised by completely empty fibrils, was distinctly higher in comparison with the high-temperature support (Y950/FAHCL). All materials studied were very porous with the P value ranging from about 73% up to 90%. High apparent density of Y350/FAHCL was a result of the high increase in weight (137%) of a support during one-step infiltration by furfuryl alcohol (see Fig. 8). In the case of Y950/FAHCL weight of a support increased by only 22%.

Figure 9 shows the dynamic elastic moduli measured along basic directions (axial and radial) in yucca carbonised at 350 and 600 °C, and in the composites Y350/FAHCL and Y600/FAHCL. Higher values of moduli determined along axial direction than those along radial direction are indebted to strong fibres of yucca, which are aligned parallel to the stem axis. Moduli E_{ax} and E_{rad} for composites were found to

Table 1 Carbon content and the physical parameters determined for initial yucca, carbonised at 350 and 950 °C, as well as for the composites produced from those supports

Sample	Carbon content (wt.%)	d_{app} (g/cm^3)	d_{true} (g/cm^3)	P (%)	ρ_{ax} (Ω m)	ρ_{rad} (Ω m)
Raw	45.21	0.322	1.538	79.06	2.2×10^{5}	1.5×10^{6}
Carbonised at 350 °C	71.17	0.182	1.354	86.56	2.0×10^{4}	3.7×10^{4}
Carbonised at 950 °C	78.21	0.225	1.981	88.64	4.2×10^{-4}	1.4×10^{-3}
Composite Y350/FAHCL	n.d.	0.490	1.806	72.87	2.8×10^{4}	5.7×10^{4}
Composite Y950/FAHCL	n.d.	0.338	1.997	83.07	2.1×10^{-3}	1.9×10^{-2}

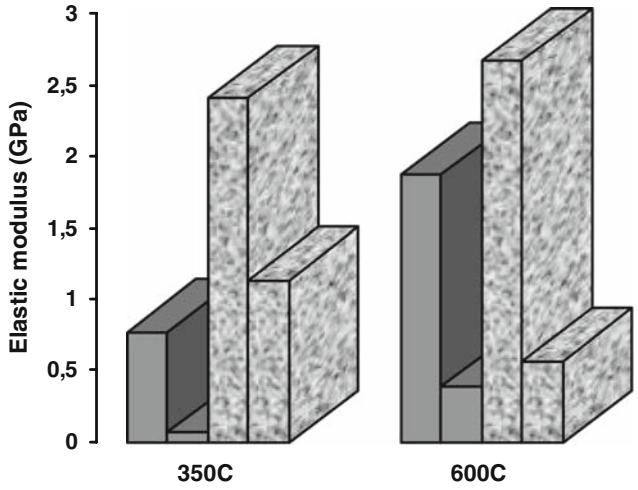

Fig. 9 The dynamic elastic moduli determined along basic directions in the support (*dark columns*) and in the composite (columns with the texture) for two temperatures of the yucca carbonisation. Left columns of each sample denote the data for axial direction; right columns for radial direction

be several times greater than those of the supports. In spite of high bulk porosity, the biomorphous block composites produced from renewable precursor using only one step of infiltration were characterised by very good stiffness with dynamic elastic moduli of order of GPa.

Table 1 presents the data of the electric resistivity, ρ, of raw yucca, supports and composites. It can be seen from Table 1 that electric resistivity of raw yucca and carbonised at 350 °C belonged to the range of insulators, while the support produced at the highest temperature studied, i.e. at 950 °C, exhibited considerably higher conductivity—resistivity decreased by 7–8 orders. Electric conductivity of samples studied was characterised by distinct anisotropy, i.e. ρ measured along axial direction (ρ_{ax}) was considerably higher than that along radial direction (ρ_{rad}). Electric resistivity of the composites was found to be strongly dependent on the electrical properties of the support—the $\rho_{ax/rad}$ values measured for supports and their composites were of the same order. Covering internal surface of the support by thin layer of carbonised cross-linked PFA increased electric resistivity, but within the same range of the ρ values. Mentioned above is clearly seen in the case of Y950/FAHCL, which was made on the basis of material with low electric resistivity. Probably electric resistivity of pure carbonised cross-linked PFA is of range of insulators.

X-ray diffraction studies made by Kercher and Nagle [27] for monolithic pieces of fibreboards carbonised at various temperatures evidenced the microstructural evolution occurring during charcoal carbonisation. As the carbonisation temperature, T_c, increased, the large turbostratic crystallites grew very little, while the graphene sheets grew substantially. At about 900 °C, the large graphene sheets and the large turbostratic crystallites (conductive phases) impinged on each other. Increasing impingement of crystallites with increasing T_c was suggested to be responsible for the nonmetal–metal transition of carbon materials. The graphitisation behaviour of carbonised pure plant, i.e. of bamboo, after high-temperature heat treatment was investigated by Cheng et al. [26]. Experimental results showed that the d_{002} spacing of the bamboo carbon decreased and the apparent graphite crystallite size increased with increasing graphitisation temperature. However, even after heat treatment at 3000 °C, the crystallite size was only about 9 nm. The other technique, i.e. TEM, also allows to observe the ordering of a structure and gives the crystallites sizes. Figure 10 shows the 002DF TEM images of two kinds of yucca carbonised at two limit temperatures, 350 and 950 °C. They are characterised by poorly developed structure. Yucca carbonised at both temperatures shows mostly the disordered phase, that is carbon phase only in approximation (carbon content in carbonised yucca depended on T_c and it was ~71 and ~78 wt.%, respectively). Ordered structural areas of small sizes <10 nm are noticeable mainly on the edge of the grain. Increase of carbonisation temperature increases number of these ordered areas, although degree of the yucca structure ordering becomes still inconsiderable. Distinct increase of about 7–8 orders in electrical conductivity in yucca carbonised at 350 and 950 °C is probably related to different mechanism than that discovered in carbonised commercial fibreboards generated from different wood fibre precursors [27].

It is known from our previously published article [20] that strong EPR signals with high concentration of paramagnetic

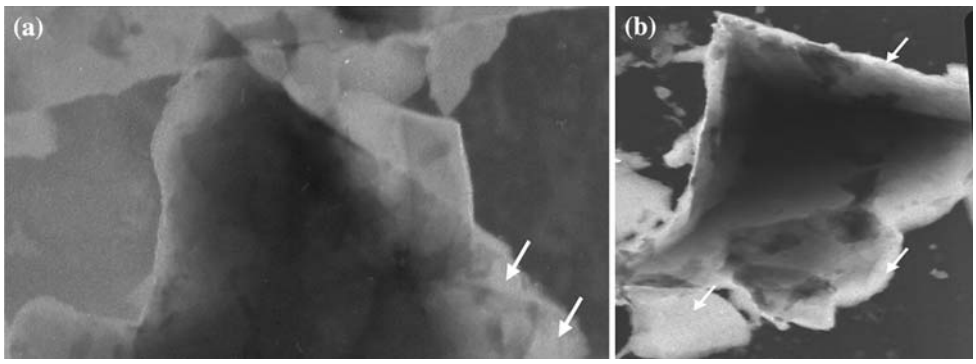

Fig. 10 TEM images (002 DF) of yucca carbonised at 350 °C (**a**) and 950 °C (**b**). White objects (shown by arrows) represent groups of crystallites orientated towards 002 direction

centres ($\sim 10^{20}$ spin/g) were characteristic for the yucca thermally decomposed at 550 °C, while yucca heated to 950 °C was described by very weak EPR lines ($\sim 10^{17}$ spin/g). The thermal decomposition of plants at lower temperatures caused breaking of chemical bonds, while heating to 950 °C transformed the plant structure to system with saturated bonds. It is clear that for the composite preparation samples carbonised at lower temperatures are more suitable because of high number of not-saturated bonds. Additional advantage of using lower temperature of pyrolysis is lower energy consumption during the support preparation.

There is a serious problem in preparation of the yucca-based composites, whether an interaction between filler, i.e. PFA, and skeleton of the carbonised yucca occurs. Cheng et al. [26] used phenol resin to impregnate raw bamboo. Bamboo with reinforced cell walls with glassy carbon was heat treated in the same way as raw bamboo mentioned previously. The XRD profiles at every temperature studied within the range of 2100–3000 °C were found to be similar in shape for both charcoal and ceramics. Probably, there is no interaction between resin and plant in high temperatures or it is, but negligible. Basay et al. [28] have used furfuryl alcohol having sufficiently small and polar molecules to obtain a dimensionally stable natural wood polymer composite. They suggested that there is a chemical interaction between furfuryl alcohol and raw wood material—mainly cellulose. When the wood material is carbonised at high temperatures the cellulose is decomposed. Thus, one can expect absence of chemical reactions between PFA and skeleton of carbonised plant, especially prepared at $T_c > 350$ °C. But it is impossible to say categorically that this interaction does not exist. Further studies are needed to explain physical phenomena and possible chemical reactions that may occur in the yucca-based composites.

Conclusions

The biomorphous composites were produced by one-step infiltration of furfuryl alcohol into monolithic blocks of yucca, previously carbonised at temperatures between 350 and 950 °C. They were found to be light, very porous, thermo-resistant (in oxygen-absent atmosphere) carbon materials with stiff, hierarchically ordered structure. Similarly to composites made of compressed-expanded graphite as a support, these eco-friendly composites were found to be monoliths comprising a backbone, i.e. carbonised yucca skeleton, coated with a thin layer of a filler—carbonised cross-linked PFA. Electrical resistivity of composites was found to be strongly dependent on the electrical properties of the support. Covering internal surface of the conductive carbonised plant with a thin layer of the filler, being probably an insulator, increased electrical resistance.

Acknowledgements The authors gratefully acknowledge Mrs. Sylwia Czajkowska for supplying the thermogram of TGA. The main organic components of yucca were determined in the Institute of Organic Chemistry, Bulgarian Academy of Sciences, Sofia, Bulgaria. The TEM observations were made thanks to kindness of Silesian University, Department of Earth Sciences, Sosnowiec, Poland.

References

1. Rambo CR, Cao J, Sieber H (2004) Mater Chem Phys 87:345. doi:10.1016/j.matchemphys.2004.05.031
2. Sun B, Fan T, Zhang D et al (2004) Carbon 42:177. doi:10.1016/j.carbon.2003.10.008
3. Mizutani M, Takase H, Adachi N et al (2005) Sci Technol Adv Mater 6:76
4. Fey T, Sieber H, Greil P (2005) J Eur Ceram Soc 25:1015. doi:10.1016/j.jeurceramsoc.2004.05.008
5. Rambo CR, Cao J, Rusina O et al (2005) Carbon 43:1174. doi:10.1016/j.carbon.2004.12.009
6. Onyestyak G, Valyon J, Papp K (2005) Mater Sci Eng A 412:48. doi:10.1016/j.msea.2005.08.050
7. Liu Z, Fan T, Zhang W et al (2005) Micropor Mesopor Mater 85:82. doi:10.1016/j.micromeso.2005.06.021
8. Kim Y-J, Lee B-J, Suezaki H et al (2006) Carbon 44:1592. doi:10.1016/j.carbon.2006.02.011
9. Luo M, Gao J, Zhang X et al (2007) Mater Lett 61:186. doi:10.1016/j.matlet.2006.04.027
10. Li J, Shi X, Wang L et al (2007) J Colloid Interface Sci 315:230. doi:10.1016/j.jcis.2007.06.065

11. Wang Q, Jin GQ, Wang DH et al (2007) Mater Sci Eng A 459:1. doi:10.1016/j.msea.2007.02.063
12. Ghanem H, Kormann M, Gerhard H et al (2007) J Eur Ceram Soc 27:3433. doi:10.1016/j.jeurceramsoc.2007.02.197
13. Byrne CE, Nagle DC (1997) Carbon 35:267. doi:10.1016/S0008-6223(96)00135-2
14. Singh M, Martinez-Fernandez J, de Arellano-Lopez AR (2003) Curr Opin Solid State Mater Sci 7:247. doi:10.1016/j.cossms.2003.09.004
15. Halada K (2003) Curr Opin Solid State Mater Sci 7:209. doi:10.1016/j.cossms.2003.09.007
16. Hirose T, Zhao B, Okabe T et al (2002) J Mater Sci 37:3453
17. Sudin R, Swamy N (2006) J Mater Sci 41:6917
18. de Souza Rodrigues C, Ghavami K, Stroeven P (2006) J Mater Sci 41:6925. doi:10.1007/s10853-006-0217-2
19. Tokoro R, Vu DM, Okubo K et al (2008) J Mater Sci 43:775. doi:10.1007/s10853-007-1994-y
20. Krzesińska M, Pilawa B, Pusz S et al (2006) Biomass Bioenergy 30:166. doi:10.1016/j.biombioe.2005.11.009
21. Krzesińska M, Zachariasz J (2007) J Anal Appl Pyrol 80:209. doi:10.1016/j.jaap.2007.02.009
22. Krzesińska M, Zachariasz J (2007) J Phys: Conf Ser 79 Paper No. 012012
23. Krzesińska M, Zachariasz J, Muszyński J et al (2008) Bioresour Technol 99:5110. doi:10.1016/j.biortech.2007.09.050
24. Celzard A, Krzesińska M, Begin D et al (2002) Carbon 40:557. doi:10.1016/S0008-6223(01)00140-3
25. Krzesińska M, Zachariasz J (2007) J Phys: Conf Ser 79 Paper No. 012011
26. Cheng HM, Endo H, Okabe T et al (1999) J Porous Mater 6:233. doi:10.1023/A:1009684014651
27. Kercher AK, Nagle DC (2003) Carbon 41:15. doi:10.1016/S0008-6223(02)00261-0
28. Basay E, Ozaki SK, Yalinkilic MK (2004) Wood Sci Technol 38:405